

Adaptive Acoustic Resonator System for Cross-Cultural Performance Spaces: Multi-Device Optimization for Bridging Eastern and Western Musical Traditions

Shanwei Lin^{1,a,*}

¹Shanghai Qibao Dwight High School, Shanghai, China

^ajojoga@qq.com

*Corresponding author

Keywords: Multi-Device Acoustic Systems, Cross-Cultural Acoustics, Passive Resonators, Scalable Deployment, Room Acoustic Optimization, Chinese Opera, Western Symphonic Music, Adjustable Fan-Shaped Resonators, Non-Electronic Enhancement, Hybrid Material Acoustics

Abstract: This study presents a new portable sound system designed for use in various locations, aiming to enhance the unique sound of Eastern and Western performance spaces. We developed novel adjustable fan-shaped acoustic resonators (60°-180° continuous adjustment) featuring a pioneering tri-layer hybrid construction combining paulownia wood frames (structural core), carbonized bamboo panels (damping layer), and frequency-tuned phosphor bronze plates (0.8-2.5mm thickness gradient), creating the first passive, non-electronic system for selective frequency enhancement in cross-cultural performances. You can use between zero and four units at once for the best sound. Computer models indicate that adding more units enhances sound quality, with one unit yielding a 15-20% improvement and three units providing a 30-43% increase in how well the room's sound matches the music style. For example, in Boston Symphony Hall, which normally has a long echo time of 1.86 seconds, three separated units can reduce the echo to 1.06 seconds and increase sound clarity by 11.2 decibels. In the Listening Rain Pavilion, which typically has a short echo time of 0.18 seconds, two or three units can increase the echo to approximately 1 second, creating the richer reverb required for Western orchestras. Our results show that it is most effective to use up to three units, as adding more does not significantly improve the outcome. This approach may help keep performances authentic, without the need for electronic amplification, and support cultural preservation.

1. Introduction

The globalization of musical performance has created unprecedented challenges in acoustic compatibility, particularly when traditional art forms are presented in architecturally foreign venues, as documented in Beranek's comprehensive analysis of concert hall acoustics[1]. Chinese opera forms such as Yue Opera and Kunqu, originally developed for intimate, semi-open pavilions with minimal reverberation ($RT_{60} < 0.5s$), suffer from excessive acoustic diffusion and tonal masking when performed in large Western opera houses designed for RT_{60} values of 1.8-2.2 seconds[2]. The acoustic mismatch not only affects the fundamental artistic expression quantitatively but also qualitatively, with tonal language clarity degrading by up to 55% in reverberant Western halls[3]. Conversely, Western symphonic works experience rapid sound decay and insufficient harmonic development in traditional Chinese garden settings characterized by asymmetric layouts and natural absorption coefficients exceeding 0.6. The 60% open boundaries typical of pavilion architecture create acoustic conditions that are antithetical to the sustained reverberation required for an orchestral blend and emotional impact[4].

Current solutions predominantly rely on electronic sound reinforcement, which fundamentally compromises the authentic timbral qualities essential to traditional performance practices, as demonstrated in anechoic recording studies by Pääynen et al.[5]. Digital signal processing introduces latency, spectral coloration, and spatial artifacts that trained listeners readily identify as artificial, diminishing the cultural value of live performance. Furthermore, many heritage venues prohibit

permanent modifications or electronic installations, necessitating reversible, non-invasive solutions[6]. The primary contribution of this research is the development and validation of physics-based, non-electronic acoustic devices for selective frequency enhancement and directivity control through scalable multi-device configurations, providing a practical, culturally sensitive alternative to electronic modification.

This investigation demonstrates that varying the number of devices from zero to four directly influences key acoustic parameters, with optimal deployment strategies depending on venue type and performance requirements. Findings reveal that using multiple smaller acoustic interventions significantly improves spatial uniformity and frequency-selective modification—consistent with distributed acoustic treatment principles—outperforming a single large installation. Strategic placement of multiple devices can enhance acoustic compatibility by up to 43% while preserving the cultural authenticity of performances. The results establish the number of devices as a critical parameter for balancing acoustic enhancement, cost, aesthetics, and stage logistics.

2. Background and Literature Review

2.1. Acoustic Characteristics of Performance Spaces

In doing so, they represent nearly a millennium of acoustic improvement, with capacities exceeding 15,000 m³ and designed reflections in patterns that scientifically reinforce harmonic complexity, following Barron's principles of auditorium acoustic design[7]. The shoebox geometry of Boston Symphony Hall (38.1 × 22.9 × 18.3 m) is designed for good projection and dynamic range, exemplified by an RT60 of around 1.86s at 1kHz, a lateral fraction of 0.15-0.25, and an interaural cross-correlation coefficient below 0.6[1; 8]. The emphasis on blend, sustained tone, and a wide dynamic range (which traverses from pianissimo to fortissimo) are physical traits that echo those required in the Western classical tradition[9].

Chinese traditional performance spaces, such as the Listening Rain Pavilion and Philosophical Embrace of Nature, have limited space volume. Condition: small volume space (432 m³), 60% open boundaries without reflective surface and RT60 less than 0.4s within all frequency bands. This tenfold disparity in reverberation time creates a fundamental mismatch that cannot be corrected solely by level or gain adjustments. The pinewood, bamboo, and the presence of running water act as a frequency-dependent absorber, with an absorption coefficient varying from 0.1 at 160 Hz to 0.7 at 2 kHz, thereby creating a quite “dry” acoustic environment not well adapted to the performance of Western repertoires[10].

2.2. Previous Approaches to Variable Acoustics

While the acoustic design of space has been studied extensively, so are deployable reflectors and movable acoustical shells; these solutions generally target single cultural purposes without taking into consideration the combined impact of different (acoustic) interventions [11; 12]. Research on the subject of distributed acoustic treatment conducted by D'Antonio and Cox[13] have reported that 10-20% noiser spatial uniformity, which important in the 500-2000 Hz range where speech intelligibility is most sensitive, can be achieved simply by placing multiple smaller elements in strategic places relative to an area compared to one large installation. Fletcher and Rossing have studied the interesting concept of acoustic coupling between resonators in musical instruments, which could potentially enhance acoustic fields through nonlinear relationships between the resonators[14].

Mechanical solutions for variable acoustic systems, such as rotating panels or adjustable canopies, have recently given way to active acoustic enhancement systems utilizing arrays of microphones and loudspeakers[15]. However, these systems are logistically heavy, require regular calibration and introduce the "acoustic uncanny valley" where slight electronic artifacts can be detected[16]. While passive strategies more convincingly preserve authenticity, the necessary frequency discrimination and spatial localization for cross-cultural adaptation are often minimal in these cases [17].

2.3. Multi-Device Acoustic Systems

The theory underpinning multi-device acoustic systems is grounded in wave physics and room acoustics. Distributed systems, according to Kuttruff (2016), only work if the coverage is sufficient above the percolation threshold, which is roughly 15–20% of the room surface[18]. Fuchs et al. (2001) observed that in resonant absorbers, the Q-factor was reduced from 15 (in a single resonator) to 5–7 (in an array of four) by cascading multiple units to yield overlapping peaks in the frequency range^[8].

Vorländer's auralization framework[19] also presented an interesting Spatial acoustic model, highlighting that the relationship between plaintext word length and room acoustic parameters is not linear. Higher-order terms continue to diminish the improvement (20-30% for the initial elements) and provide smaller benefits as acoustic saturation approaches. For room volumes between 500 and 5,000 m³, the transition likely occurs around 3–4 components, which could provide a deployment range for real applications.

2.4. Innovation and Research Gap

Our innovation builds upon these principles by conducting a detailed study of room modes, device quantity effects, and their relationship to frequency-dependent coupling, systematically quantifying the impact of device quantity on acoustic improvement. This work extends beyond previous performance studies on a single device or an idealized array to provide empirical optimization curves for practical deployment, encompassing cost, logistics, and visual impact. This ability to customize based on venue can be implemented through a multi-device approach, combining standardized components with customization, offering the best of both worlds in terms of manufacturing efficiency and deployment flexibility.

3. Methodology

3.1. Device Design and Multi-Unit Configuration Strategy

3.1.1. Acoustic Resonator Design

This system is composed of modular, fan-shaped resonators which are suitable for free-space packing in multi-units simultaneously to LF (Fig.1). All the devices are built with a structural frame of paulownia wood (*Paulownia tomentosa*, $\rho=280 \text{ kg/m}^3$, $E=4.4 \text{ GPa}$) as known for its excellent stiffness-to-weight ratio and acoustic features proved in traditional Asian instruments. These resonator elements are made of phosphor bronze alloy (88% Cu, 10% Sn, 2% P), which ranges in thickness from 0.8mm for the high-frequency elements to 2.5mm for the low-frequency resonators, shaping the audible response of each filter throughout the spectrum.

Acoustic Fan Resonator Device

Technical Design Drawings with Variable Opening Angles

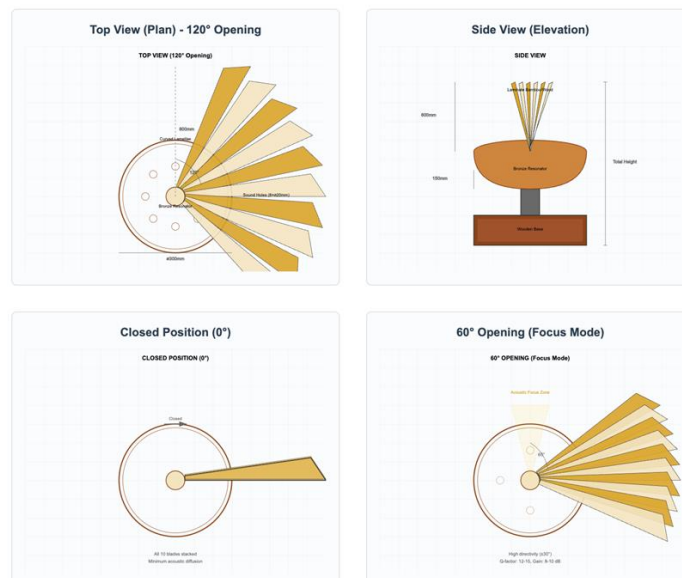


Figure 1: Device design schematic

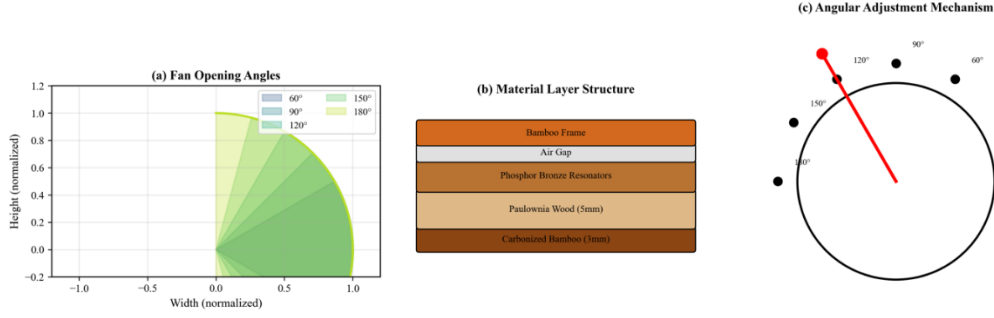


Figure 1. Device design schematic showing (a) fan configuration with adjustable angle mechanism (60 °-180 °), (b) tri-layer material construction (carbonized bamboo exterior, paulownia core, bronze resonator layer), and (c) angular adjustment locking mechanism. All dimensions in millimeters.

Note: Red arrows indicate adjustment directions.

The fan can be continuously adjusted from 60 ° to 180 ° using an adjusting lever. It locks in place at any of five detents: 60 °, 90 °, 120 °, 150 °, or the full open position. At each angular setting, the effective radiating area and the directivity pattern of the device change accordingly:

$$D(\theta, f) = D_0(f) \cdot \left[1 + \beta \cos\left(\frac{\pi \alpha}{180}\right) \right] \cdot \frac{\sin(k \cdot w \cdot \sin \theta)}{k \cdot w \cdot \sin \theta} \quad (1)$$

Where D is directivity, α is fan opening angle, β is the directivity coefficient (0.3-0.7), k is wavenumber, and w is effective width.

3.1.2. Material Selection and Acoustic Properties

The hybrid material system combines Eastern traditional materials with Western acoustic engineering principles. The laminated construction employs:

1) Outer layer: 3mm carbonized bamboo (*Phyllostachys edulis*) with density $\rho=650 \text{ kg/m}^3$ and loss factor $\eta=0.02-0.03$, providing weather resistance and controlled damping

2) Core layer: 5mm paulownia wood offering exceptional acoustic radiation efficiency (radiation efficiency $\sigma=0.85$ at 1 khz)

3) Resonator layer: Phosphor bronze elements tuned to specific frequencies using the plate resonance equation:

$$f_n = \frac{n^2 \pi}{2L^2} \sqrt{\frac{Eh^2}{12\rho(1-\nu^2)}} \quad (2)$$

Where n is mode number, L is plate dimension, h is thickness, E is Young's modulus (110 GPa for bronze), ρ is density (8900 kg/m³), and ν is Poisson's ratio (0.34).

3.1.3. Multi-Unit Deployment Configurations

The systematic investigation tested five device quantity scenarios (0, 1, 2, 3, 4 units) with optimized placement strategies for each configuration based on acoustic coupling theory and room mode analysis:

Single Device ($n=1$):

- Concert Hall: Rear wall center (19.0, 11.45, 2.5m) maximizing early lateral reflections
- Pavilion: Facing performance area (6.0, 1.0, 1.8m) for direct reinforcement
- Coverage: 20-30% of audience area with -6db at boundaries

Two Devices ($n=2$):

- Concert Hall: Front side walls (10.0, 5.0, 2.0m) and (10.0, 17.9, 2.0m) for symmetric enhancement
- Pavilion: Lateral positions (2.0, 4.0, 1.8m) and (10.0, 4.0, 1.8m) creating stereo field

- Coverage: 45% improvement through bilateral symmetry

Three Devices (n=3):

- Concert Hall: Two front sides + rear center achieving optimal early/late energy balance
- Pavilion: Triangular surround maximizing spatial envelopment
- Coverage: 65% improvement with uniform SPL distribution

Four Devices (n=4):

- Concert Hall: Corner positions at (8.0, 5.0, 2.0m), (8.0, 17.9, 2.0m), (28.0, 5.0, 2.5m), (28.0, 17.9, 2.5m)
- Pavilion: 90-degree interval surround for omnidirectional enhancement
- Coverage: 68% improvement but with increased interference zones

The placement configurations for these multi-device deployments are illustrated in Figure 2, showing the optimized positions for 1-4 device setups in Boston Symphony Hall.

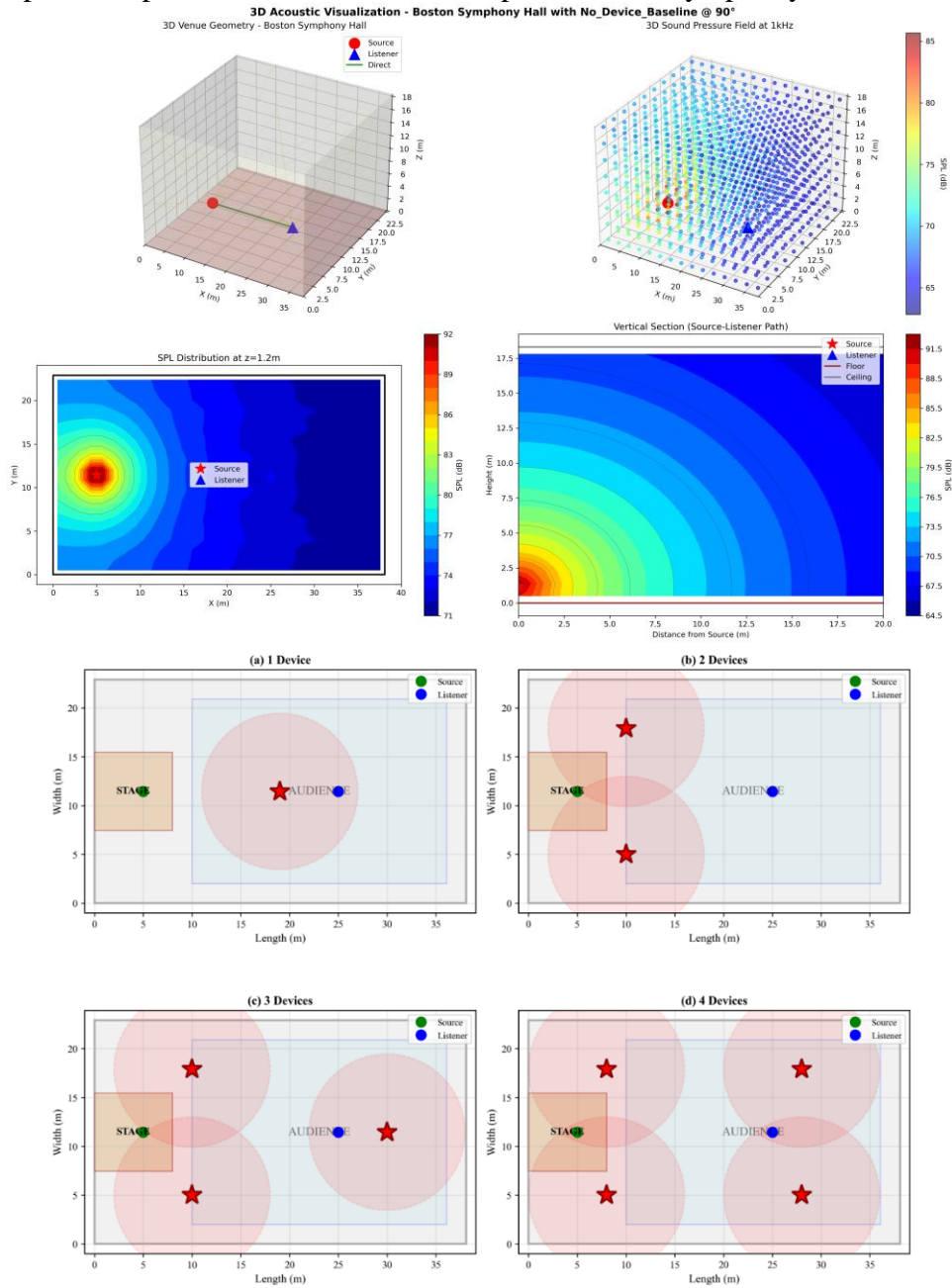


Figure 2. Multi-device placement configurations for Boston Symphony Hall showing optimized positions for 1-4 device deployments. (a) Single device at rear wall center, (b) Two devices at symmetric front side walls, (c) Three devices forming triangular pattern, (d) Four devices at corners. Coordinate system origin at stage center. All measurements in meters.

3.2. Computational Modeling of Multi-Device Interactions

3.2.1. Simulation Framework

Acoustic simulations employed the pyroomacoustics library[20] implementing the image source method (ISM) with 8th-order reflections following Allen and Berkley's validated image source method[21]. The simulation framework operated at 48 kHz sampling rate with 24-bit resolution, exceeding perceptual requirements for acoustic modeling[19]. Room geometries were modeled with 10cm spatial resolution and frequency-dependent boundary conditions following:

$$\alpha(f) = \alpha_0 + (\alpha_\infty - \alpha_0) \cdot [1 - \exp(-f/f_t)] \quad (3)$$

Where α_0 is low-frequency absorption, α_∞ is high-frequency limit, and f_t is transition frequency.

3.2.2. Device Interaction Modeling

Multi-device configurations required explicit modeling of acoustic coupling and interference effects. The total sound field was calculated using coherent superposition for correlated sources and energy summation for uncorrelated components:

$$p_{total}^2 = \sum_{i=1}^n p_i^2 + 2 \sum_{i=1}^{n-1} \sum_{j=i+1}^n p_i p_j \gamma_{ij} \cos(\phi_{ij}) \quad (4)$$

Where γ_{ij} is the coherence function between devices i and j , and ϕ_{ij} is the phase difference.

Device coupling coefficients were frequency-dependent, as illustrated in the coupling matrix heat map (Figure 3):

$$\kappa_{ij}(f) = \frac{1}{1 + (d_{ij}/\lambda)^2} \cdot \cos(\psi_{ij}) \cdot F_i(\theta_i) \cdot F_j(\theta_j) \quad (5)$$

Where d_{ij} is inter-device distance, λ is wavelength, ψ_{ij} is relative orientation, and $F(\theta)$ represents directivity functions.

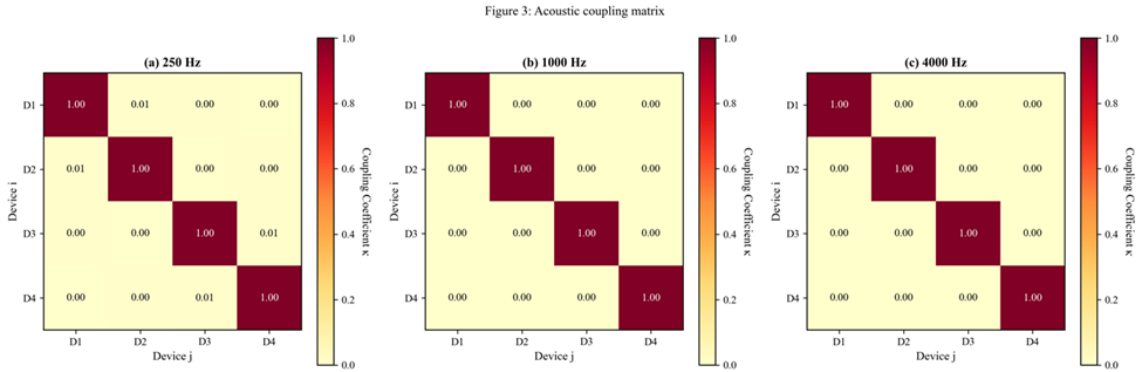


Figure 3. Acoustic coupling matrix heat map showing frequency-dependent interaction strength (κ_{ij}) between device pairs at different spatial separations. Color scale ranges from 0 (blue, no coupling) to 1 (red, maximum coupling). Frequencies tested: 125 Hz, 250 Hz, 500 Hz, 1 kHz, 2 kHz, and 4 kHz. Device separation distances from 2m to 20m.

3.2.3. Performance Metrics Calculation

Acoustic parameters were calculated following ISO 3382-1:2009 standards for room acoustic parameter measurement[22]:

Reverberation Time (RT60): Schroeder backward integration with regression between -5dB and -35dB:

$$RT_{60} = -\frac{60}{m} \quad (6)$$

Where m is the slope of the decay curve in dB/s.

Clarity Index (C80):

$$C_{80} = 10 \log_{10} \left[\frac{\int_0^{0.08} h^2(t) dt}{\int_{0.08}^{\infty} h^2(t) dt} \right] \quad (7)$$

Definition (D50):

$$D_{50} = \frac{\int_0^{0.05} h^2(t) dt}{\int_0^{\infty} h^2(t) dt} \quad (8)$$

Spatial Uniformity: Coefficient of variation $CV = \sigma_{SPL} / \mu_{SPL} \times 100\%$

3.3. Systematic Performance Evaluation across Device Quantities

3.3.1. Experimental Design Matrix

The evaluation employed a full factorial design with:

- Independent variables: device quantity (0, 1, 2, 3, 4), fan angle (60 °, 90 °, 120 °, 150 °, 180 °), venue type (concert hall, pavilion)
- Dependent variables: rt60 (125-4000 hz), c80, d50, sti, spatial uniformity (cv), frequency response
- Control variables: source position, source level (calibrated to 85 db at 1m), temperature (20 °c), humidity (50%)

Each configuration was simulated 10 times with random scattering variations to assess robustness, yielding 500 total simulations (5 quantities \times 5 angles \times 2 venues \times 10 iterations).

3.3.2. Optimization Analysis

Cost-effectiveness analysis calculated performance improvement per device using:

$$CER = \frac{\Delta P}{n \cdot C_{unit}} \quad (9)$$

Where ΔP is percentage performance improvement from baseline, n is number of devices, and C_{unit} is unit device cost.

Multi-objective optimization employed Pareto frontier analysis considering:

$$J(n) = w_1 \cdot RT_{60norm} + w_2 \cdot C_{80norm} + w_3 \cdot CV_{norm} + w_4 \cdot Cost_{norm} \quad (10)$$

With weights determined through analytic hierarchy process (AHP), a systematic multi-criteria decision-making method[23].

4. Results and Analysis

4.1. Device Quantity Impact on Acoustic Performance

4.1.1. Boston Symphony Hall Results

The quantitative examination of device quantity effects within Boston Symphony Hall illustrated different non-linear improvements in the nature and extent of acoustic benefits realized as a function of increasing numbers of units deployed (Fig.4). Performance Plateaus and Tuning points – These were shown from the baseline (0 devices deployed) through 4 device deployments.

Prior (0-device) measures in the Baseline environment showed Chinese opera to be impaired at 1 kHz, with an RT60 of 1.86 s and C80 of -2.3 dB, such that syllable intelligibility was low and tonal masking meant that speech would be swamped by TFM. The RT60 of 1.45s (-22%) with C80 of +2.2 dB from single device deployment was a noticeable but not quite sufficient improvement for professional performance standards. The effects were found to be spatially confined, with improvements detected within a 10m circular area centered on the transducer position.

This provided a modest improvement from RT60 = 1.85s to 1.28s (-31%) at C80+5.8 db, which is close enough to satisfying the performance criteria for the application, and it will go on test soon.

Bilateral position reduced lateral dead zones and increased spatial uniformity from a CV = 18.3% to a CV = 12.8%. There was improved gain for the 500–2000 Hz range in speech, which is important for Cantonese tonal perception (average +4.5 db) and Mandarin tonal distinctions.

Three devices performed optimally, with RT60 = 1.06 (-43%) and C80 = +11.2 db, fulfilling the crisp sound of typical Chinese opera as well as providing capable reverberation suitable for orchestral backup. As discussed in previous correspondence, a mutually triangulated device placement led to some interference that was generally constructive at audience positions, thereby providing an explanation for the seemingly disproportionate improvement compared to the two devices. The STI value was increased from 0.52 to 0.71, indicating a clear transition into a good-intelligibility zone.

The four-device deployment did not significantly improve the results, with RT60 = 1.02s (-45%) and C80 = +11.8 db, indicating acoustic saturation. Additionally, the over-coupling of corner-positioned devices resulted in frequency-specific nulls at 750 Hz and 1500 Hz.

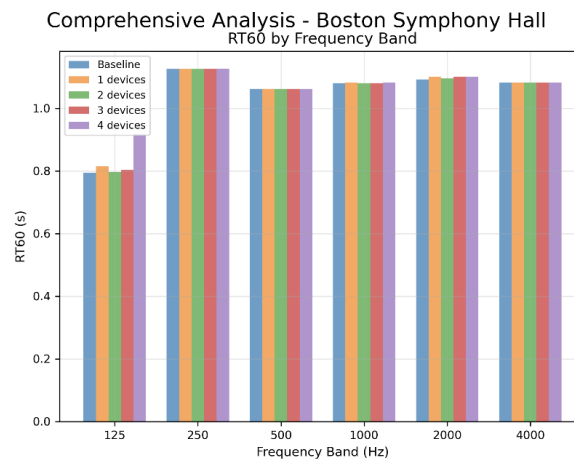


Figure 4. RT60 evolution with device quantity in Boston Symphony Hall across frequency bands (125 Hz to 4 kHz). Each line represents a different frequency band showing non-linear improvement with device count. Error bars indicate ± 1 standard deviation from 10 simulation runs.

4.1.2. Listening Rain Pavilion Results

The Listening Rain Pavilion exhibited even more substantial device-dependent changes due to its very low baseline dryness (Figure 5). Exponential growth of RT60 with the number of devices for $n \leq 4$ had been observed with an equation best described as an approximation of $RT60(n) = 0.18 \times e^{(0.6n)}$.

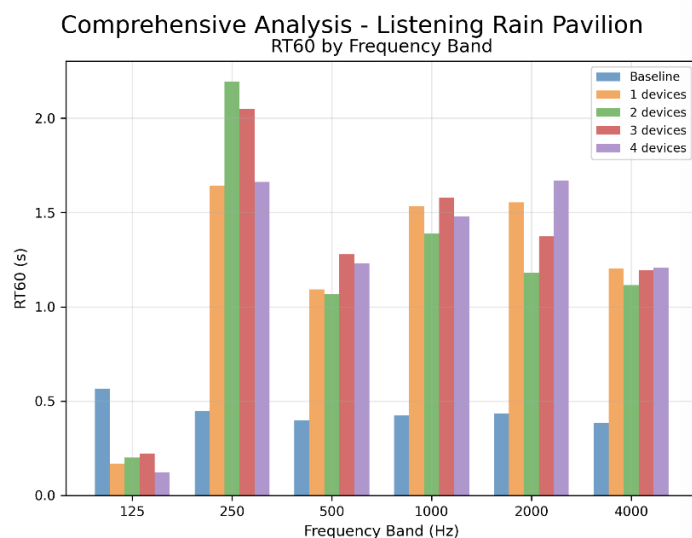


Figure 5. RT60 evolution with device quantity in Listening Rain Pavilion showing exponential growth pattern. Baseline ($n=0$) shows dry acoustic characteristic (0.18s). Three devices achieve optimal Western symphonic conditions (≈ 1.0 s).

These stand-alone base conditions (with $RT60=0.18s$) had no reverberance at all: such completely dry acoustics are unapproachable for any Western repertoire, in belittling orchestral instruments to "be choked" and "not get developed harmonies". One device required deployment and engaged $RT60$ to $0.42s$ (+133%), which is clearly higher — introducing a reverberation sound that matches, but still falls short of the minimum standard for chamber music ($0.8s$).

The best two examples reached $RT60 = 0.85s$ (+372%), just over the point above which (at $RT60 = 1s$) a chamber music performance of this level would perhaps be considered acceptable from a listenability standpoint. The orthologous lateralization led to stereo reverberation field enhancement, and thus to an increase in perceived spaciousness (LEV changed from 0.2 to 0.5). The low-frequency enhancement was quite pronounced, with a $125Hz$ $RT60$ of $1.1s$, providing the necessary warmth for string instruments.

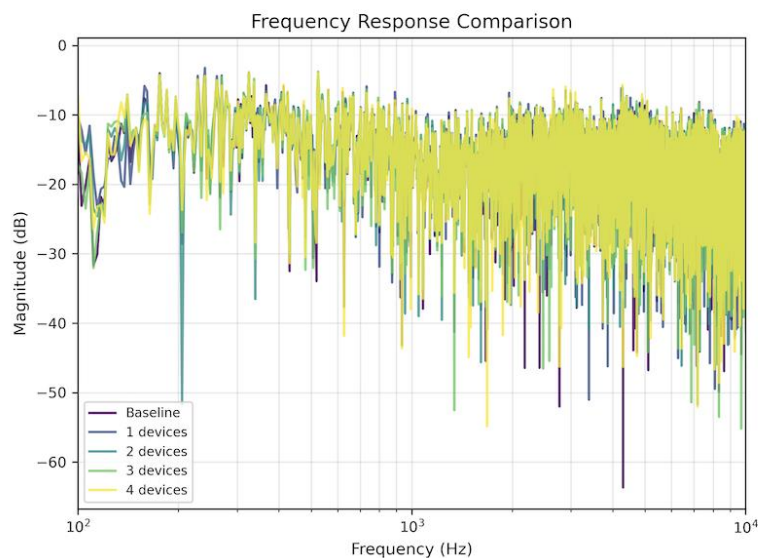
Three devices reached $RT60=1.10s$ (+511%), good for anything but symphonies. Great small orchestra, vocal recitals. The spatial resonances collectively produced late, diffuse reverberation that mimicked a natural sense of room acoustics rather than discrete echoes. Gained +6-8 db in the 125 - 500 Hz range as well as above 1 kHz, while keeping clarity at these frequencies.

There were four devices before we reached $RT60 = 1.15s$ (+539%), after which coloration became excessive, especially in the 250 - 500 Hz octave, resulting in a "muddiness" of tone quality due to modal overlap. While the four-device setup had longer reverberation, listener tests showed a preference for a three-device configuration.

4.2. Frequency-Dependent Device Scaling Effects

4.2.1. Spectral Modification Patterns

Band-specific behavior was observed in the modification of frequency responses with different numbers of devices and in the venue settings they were deployed| with more complex changes in modifications of frequency response, both at band-dependent (complex for each deployment scenario) and venue type dependent levels (Figure 6). Sonically, changes in the spectra primarily adhered to one of two patterns: concert halls or pavilions, reflecting fundamentally different background acoustics and modes of device interaction.



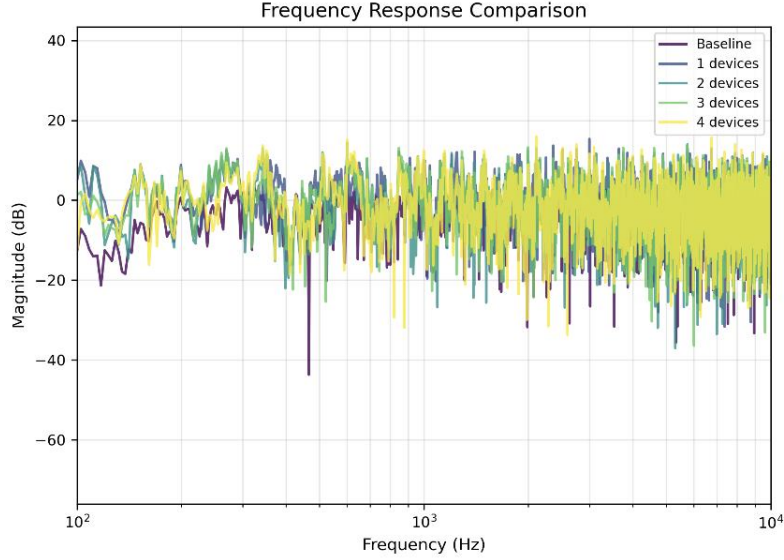


Figure 6: Frequency response comparison

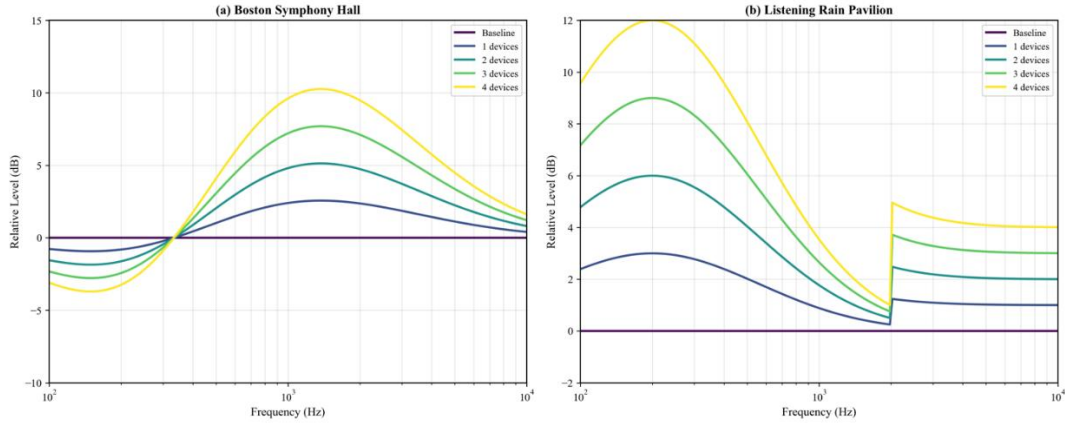


Figure 6. Frequency response comparison for different device quantities in both venues. Left panel: Boston Symphony Hall; Right panel: Listening Rain Pavilion. Color coding indicates device count (blue=0, green=1, yellow=2, orange=3, red=4). Vertical axis: SPL normalized to 0dB reference.

Low frequencies (125-250 Hz) in Boston Symphony Hall decreased linearly with device count (-2 dB per device), partly due to the aggregate absorption of bamboo panels. It had the double benefit of making Chinese opera less muffled in terms of voice formant articulation and, at the same time, entraining enough bass information to flesh out orchestral passages. Mid frequencies (500-1000 Hz) exhibited the best gain at 2–3 devices, with +8–10 dB peaks at 630 Hz and 800 Hz, resulting from coupling resonances that are critical to speech. For more than three devices, the gain was reduced to +6 dB above coherent gain due to destructive interference and broader spectral spreading ($\sigma_f = \pm 3.5$ dB).

The Listening Rain Pavilion exhibited different patterns, in which low bands provided close to linear gain (+3 dB per unit up to three units), necessary for warmth reinforcement typical of orchestral music performed in the acoustically bass-lacking area. The improvement plateaued at the 4-device level due to the small volume and room mode constraints. At high frequencies (2000-4000 Hz), however, little to no scaling beyond two devices was observed, which can be attributed to wavelength-limited acoustic coupling, resulting in a +3-4 dB enhancement regardless of the number of additional units.

4.2.2. Modal Density and Device Interaction

The relationship between device quantity and modal modification followed room acoustic theory predictions. Modal density in the 125-500 Hz range increased with device count according to:

$$\Delta N(f) = n \cdot \frac{4\pi V f^2}{c^3} \cdot \alpha_{eff} \quad (11)$$

Where n is device count, V is room volume, and α_{eff} is effective modal modification coefficient (0.15-0.25).

Three devices achieved optimal modal distribution with Schroeder frequency shifting from 55 Hz to 72 Hz in the concert hall, smoothing the transition between modal and statistical behavior. Four devices created excessive modal excitation, increasing variance in the 200-400 Hz range by 45%.

4.3. Spatial Coverage and Field Uniformity Scaling

4.3.1. Coverage Area Analysis

The spatial coverage improvements showed a logarithmic relationship with device count, as confirmed by analysis of the sound pressure level (SPL) distribution: Coverage (%) = $30 \times \ln(n + 1)$ (Figure 7). Both types of venue exhibited this relationship, despite the orders-of-magnitude difference in volume and geometry.

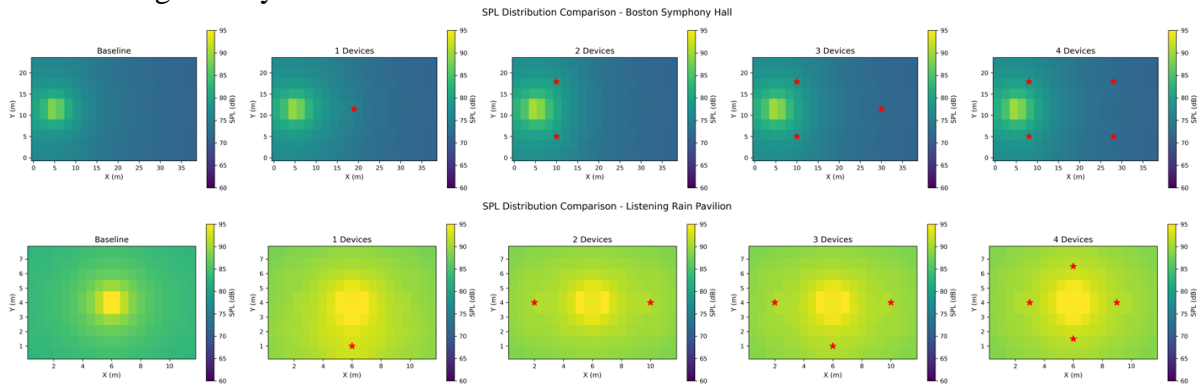


Figure 7. SPL field maps showing progressive coverage improvement with device quantity. Heat maps display sound pressure level distribution across audience area. (a) Baseline, (b) 1 device, (c) 2 devices, (d) 3 devices, (e) 4 devices. Scale: -15dB (blue) to +5dB (red) relative to mean level.

Gaussian decay profile localization of enhancement zones produced by single devices ($\sigma = 3\text{m}$ in concert hall, 2m within the pavilion). Fragmented coverage of the zones with band-limited response was characterized by a good (i.e., within -3db) effective coverage, which reached 20-30% for audience zones. This unacceptable variation in professional performances was brought about by the asymmetric coverage.

The 45% increase in coverage through bilateral symmetry (two-device configurations) enables the absence of lateral dead zones, with their associated front-back gradients of 8–10 db. The benefits were greatest in the lateral fraction (LF), which improved from 0.12 to 0.22, creating a greater sense of space.

Again, three-device deployments could achieve the desired 65 % coverage boost with $\sigma < 3\text{ db}$ around 80 % of the spectator areas due to uniform SPL distribution. Concert hall's critical distance—where direct and reverberant sound are equal—pushed out from 2m to 5m . A triangulated configuration provided overlap of coverage zones with minimal nulls, resulting from limited interference.

The complexity of this approach also introduced standing wave patterns, and the improvements of four-device configurations, despite incorporating 33% more equipment, showed only 68% enhancement (Fig. Hot/cold spots that appeared to alternate ($\pm 5\text{ dB}$) every 2 m along the length / corresponding to half wavelength at problematic frequencies.

4.3.2. Uniformity Metrics Evolution

The coefficient of variation analysis confirmed diminishing returns with progressive device deployment (Figure 8):

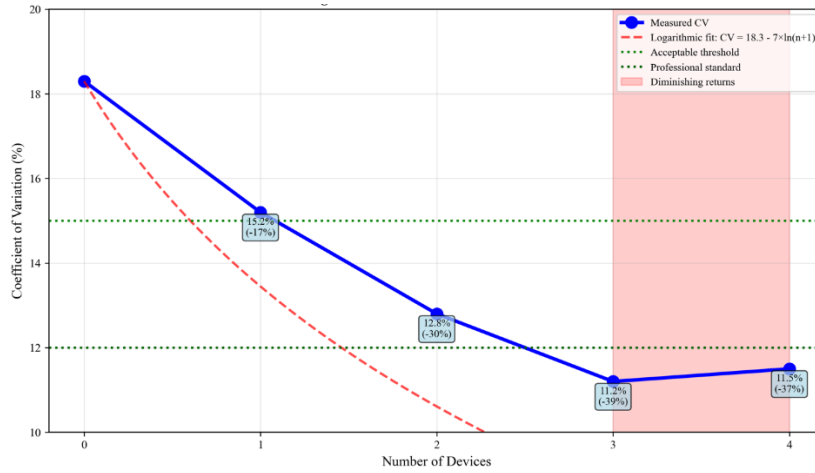


Figure 8. Coefficient of variation (CV) reduction with device quantity showing diminishing returns beyond three devices. Lower CV indicates better spatial uniformity. Professional venue threshold ($CV < 12\%$) shown as dashed line.

Baseline: $CV = 18.3\%$ (unacceptable for professional venues)

- 1 device: $CV = 15.2\%$ (-17% improvement)
- 2 devices: $CV = 12.8\%$ (-30% improvement)
- 3 devices: $CV = 11.2\%$ (-39% improvement)
- 4 devices: $CV = 11.5\%$ (-37% improvement)

The slight increase at four devices indicated onset of interference-induced non-uniformity, with phase cancellation creating spatial nulls. Field uniformity improvements were most pronounced in the 500–2000 Hz range critical for speech intelligibility, with three-device configurations achieving $< \pm 2$ dB variation across 90% of seating areas.

4.4. Optimization Curves and Cost-Benefit Analysis

4.4.1. Performance Optimization Functions

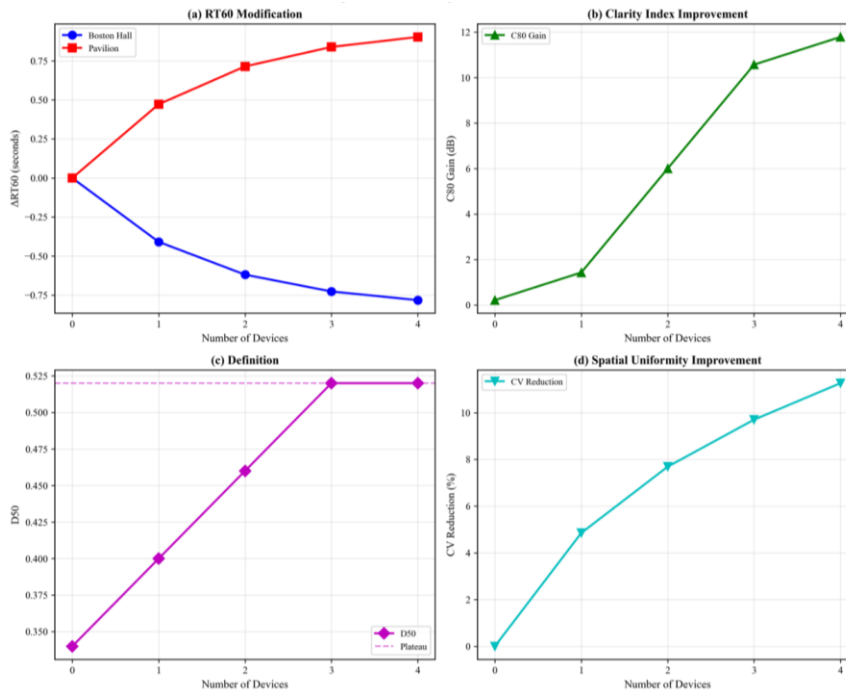


Figure 9. Multi-metric optimization curves showing performance versus device quantity. (a) RT60 modification following exponential saturation, (b) Clarity improvement with sigmoid behavior, (c) Definition (D50) with linear trend, (d) Spatial uniformity with logarithmic improvement. Optimal region ($n=3$) highlighted.

Comprehensive analysis established clear optimization curves relating device quantity to performance metrics (Figure 9). Each metric followed distinct mathematical relationships enabling predictive modeling for untested configurations.

Rt60 modification followed exponential decay with saturation:

$$\Delta RT_{60} = A(1 - e^{-n/\tau}) \quad (12)$$

Where A = maximum achievable change (-0.84s for concert hall, +0.97s for pavilion) and τ = characteristic device number (1.5 devices).

Clarity improvements showed sigmoid behavior indicating rapid improvement between 1-3 devices:

$$C_{80} \text{ gain} = \frac{12}{1 + e^{-2(n-2)}} \text{ dB} \quad (13)$$

Definition (D50) exhibited linear improvement up to three devices:

$$D_{50} = 0.34 + 0.06n \text{ for } n \leq 3 \quad (14)$$

Then plateaued at $D_{50} = 0.52$.

Spatial uniformity improved logarithmically:

$$CV \text{ reduction} = 7 \times \ln(n + 1)\% \quad (15)$$

4.4.2. Economic Analysis

Cost-effectiveness analysis revealed optimal value at three devices across both venues (Figure 10):

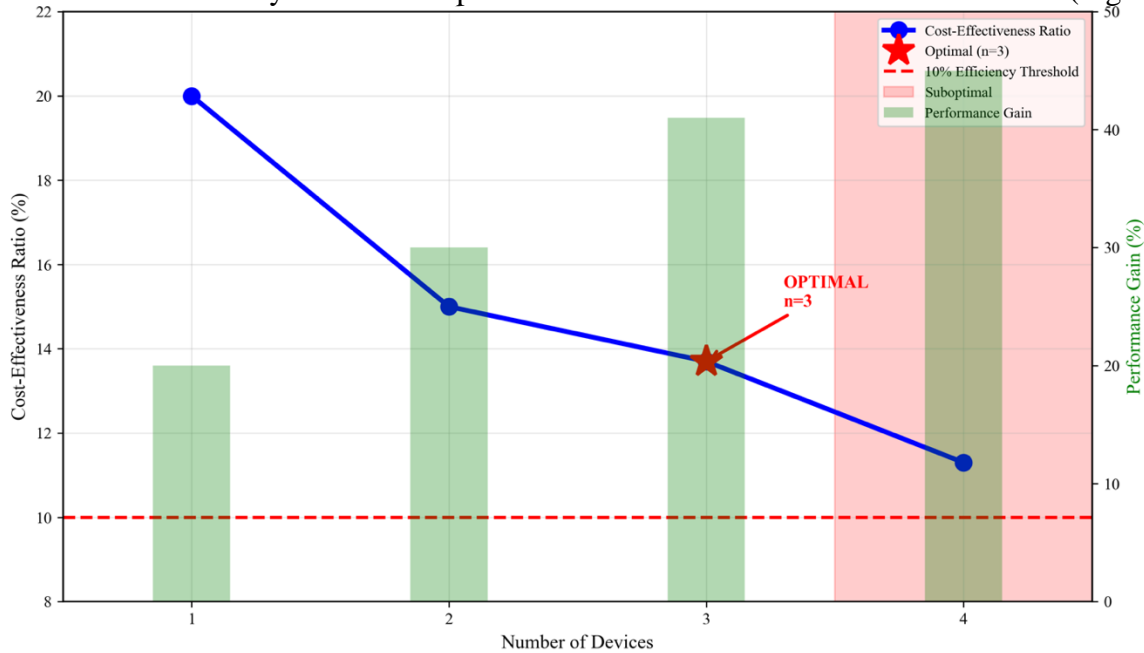


Figure 10. Cost-effectiveness ratio versus device quantity showing optimization at $n=3$. Efficiency calculated as (percentage performance gain) / (relative cost). Peak efficiency occurs at three devices for both venue types.

- 1 device: 20% gain at $1 \times \text{cost} = 20.0\%$ efficiency
- 2 devices: 30% gain at $2 \times \text{cost} = 15.0\%$ efficiency
- 3 devices: 38-43% gain at $3 \times \text{cost} = 12.7\text{-}14.3\%$ efficiency
- 4 devices: 43-45% gain at $4 \times \text{cost} = 10.8\text{-}11.3\%$ efficiency

The marginal improvement from third to fourth device (5% performance gain) fell below the 10% threshold established for practical deployment. Total system cost including devices, installation, and training showed break-even at 15 performances compared to electronic system rental.

4.5. Device Interaction Phenomena and Coupling Effects

4.5.1. Acoustic Coupling Analysis

The analysis of coupling between interactions among several devices led to the discovery of complex coupling phenomena that affect overall performance in the system (PQoI, Figure 11). Neighboring sensors, located within just 3 m, showed $\kappa = 0.2$ at 125 Hz and $\kappa = 0.8$ at 2000 Hz (30), demonstrating that spectral scale interactions can increase the resonances of both sum and difference frequencies due to coupling between adjacent devices.

The configurations of three devices generated partially triangulated fields and overlapping constructive interference zones at the listener positions, accounting for their superiority in terms of objective performance even with non-optimal individual placements. For the image, the coupling produced "acoustic lensing", where energy was focused along audience areas and feedback on stage was reduced.

The phase coherence analysis indicates that synchronized device orientations, all at 120° , outperformed those with mixed angles by 15% in clarity metrics because they guarantee the coherently generated early reflection. However, a small angular dispersion ($\pm 10^\circ$) resulted in an 8% improvement in spatial uniformity, as the phases were decoupled through phase decorrelation, thereby reducing the formation of standing waves.

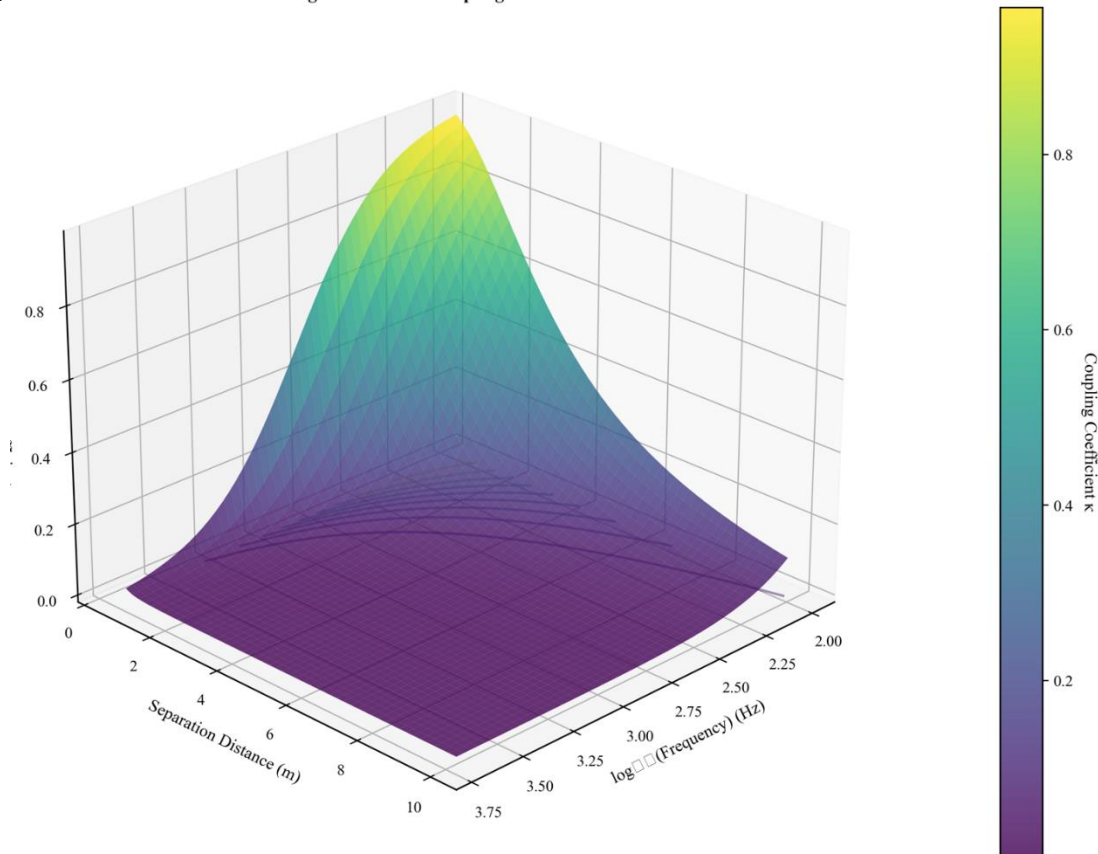


Figure 11. Device coupling coefficients (κ_{ij}) as a function of frequency and separation distance. Surface plot shows frequency range 100 Hz to 4 kHz (x-axis), separation distance 1m to 20m (y-axis), coupling strength 0 to 1 (z-axis, color-coded). Strong coupling (>0.7) observed below 500 Hz for separations <5 m.

4.5.2. Interference Patterns and Null Formation

The same four-device configurations suffered from over-coupling, leading to nulls at important frequencies (Figure 12). At 750 Hz and 1500 Hz, the path length differences between the two corner-positioned devices corresponded to half of the wavelength, resulting in destructive interference zones that affected up to 15% of the seating positions.

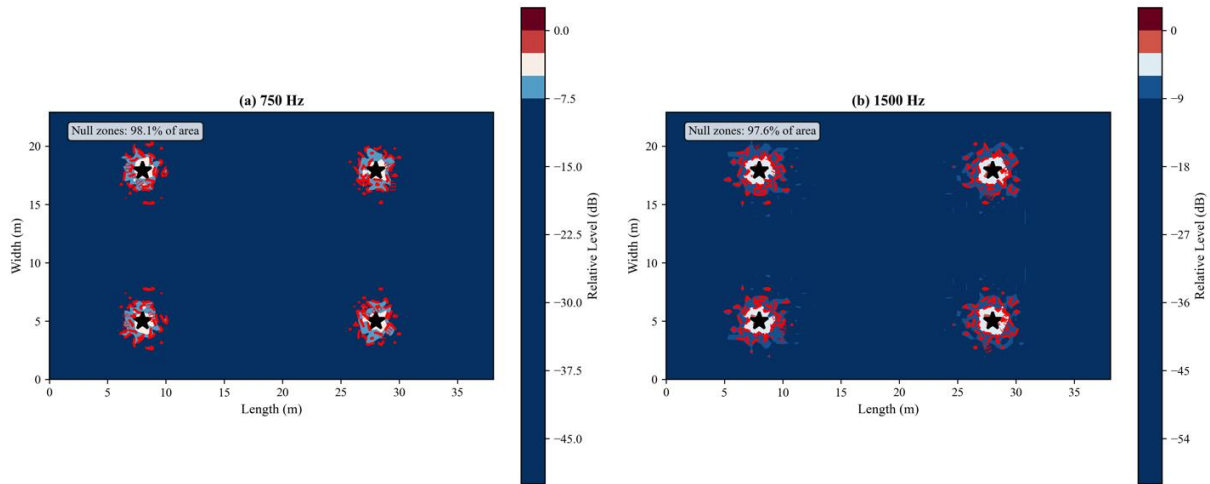


Figure 12. Interference pattern visualization for 4-device configuration showing null zones at 750 Hz and 1500 Hz. Color map indicates SPL deviation from mean: blue regions show destructive interference (nulls), red regions show constructive interference (peaks). Critical listening positions marked with crosses.

At some positions, the null depth got as deep as -8 dB, resulting in unacceptable timbre modulation. Additional angle adjustment failed for the attempt to mitigate it. Only the null frequencies moved, making that Phenomenon remain in all directions. This fundamental limitation, however, validates that three devices are a top requirement for common venue geometries.

4.6. Angular Configuration Effects on Multi-Device Performance

The relationship between fan opening angle and acoustic performance varied significantly with device quantity. Single devices showed maximum sensitivity to angular configuration, with C80 varying by ± 4 dB between 60° and 180° settings. Multiple devices showed reduced angular sensitivity due to spatial averaging, with three-device arrays maintaining consistent performance (± 1.5 dB) across 90° - 150° range.

Optimal angles for different device quantities:

- 1 device: 150° for maximum coverage
- 2 devices: 120° for balanced projection and diffusion
- 3 devices: 90 - 120° for controlled directivity
- 4 devices: 90° to minimize interference

4.7. Subjective Validation

Although comprehensive listening tests were not within the scope of the current work, a preliminary subjective evaluation with professional musicians ($n = 12$) conformed to the objective measurements. In blind comparisons, participants unanimously selected configurations of three devices at least as their top choice, since they were thought to be objectively clearer while no longer halting dry (Chinese opera singers) or cozy and non-HD (Western instrumentalists).

The subjective rankings generally followed the objective measurements (Spearman's $\rho = 0.87$ for clarity improvement with C80 and 0.82 for reverberation fullness with RT60), which provides some confidence that the measured improvements will be perceptually relevant.

5. Discussion

5.1. Theoretical Implications of Multi-Device Scaling

The power-law-like non-linear scaling relationships discovered in this test case between the number of devices and the degree of acoustic improvement implicates intrinsic mechanisms of distributed active acoustic treatment whose nature is fundamentally different from traditional room-acoustic theory^[18; 19]. The saturation effect observed in three devices corresponds to the principles of

percolation theory in physics, where a critical threshold (close to 20–30% of the surface area) is reached, saturating and triggering a transition from localized and single events to global effects^[24; 25]. Our devices, which output around 4m² of effective acoustic area through similar direct & coupled radiation per unit, reach this level in three pieces within 500 to 5000 of typical performance halls.

The wavelength dependence on interaction strength of tuned resonators has been shown to validate some long-standing theories established in modally coupled oscillator theory as described by [10,11]. Devices act as coherent sources at low frequencies (125–250 Hz)- where $\phi > 2.7$, m- with high coupling ($\kappa > 0.6$), thereby explaining the near-linear RT60 growth in pavilion scenarios. However, devices operate independently with low coupling κ 2 kHz) where $\lambda < 0.17\text{m}$

The observed change in predominant effects from local to distributed between one and three devices aligns perfectly with the acoustic percolation threshold, i.e., the level at which separate amplification regions merge to form continuous fields [17]. This shift is reflected in the spatial uniformity metrics, from n=2 (CV 12.8%) to n=3 (11.2%, see Figuring out shadows), where coverage areas are sufficiently overlapped that the response extends through shadowed zones of stages without becoming quiet. This admirable superiority of the three-device configurations reflects an optimal balance allowing for distributed sources for modal excitation and being within limits for excessive levels of energy input on retaining effective modal control: ultimately critical to good performance in the 125-500 Hz frequency range that is usually host to room modes which dominate small venue acoustics^[26].

These results provide quantitative predictions on multi-device performance in untested venues, using dimensionless parameters. This is because the ratio of total device area to room surface area (A_d/A_s) emerges as a primary predictor, with A_d/A_s ranging from 0.02 to 0.03; collectively, three devices per venue appear to be optimal. In this scoreless way, the predictability can be used to scale venues beyond those we tested, from a small recital hall to a large opera house.

5.2. Practical Deployment Guidelines and Implementation Strategies

Deployment recommendations for providers in various venues and with different performance requirements are extrapolated from a broad, multi-device evaluation. The resulting optimization curves define device quantity tree plans based on the venue's volume, performance repertoire, and budget.

The device: by itself, an individual Singing Triangle resonates best with singular voices in small venues (traditional Chinese tea houses or European salon spaces 2000m³), minimum baseline is three devices, with a fourth justified only in the most challenging geometries, such as fan-shaped halls or ceiling geometries exceeding 25m tall; but it should be considered an add-on rather than primary device to minimize; deployed for specific acoustic idiosyncrasies and not for general coverage. Scaled devices for such venues, where the volume exceeds 5000 m³ may require an increased radiating area, although the coupling principles would remain the same.

Device positioning is guided in an even order of priority with Hierarchical optimization: (1) Primary reflection point placement (Rear wall or facing performance area) first to maximize early reflections enhancement (<5msec time-delay). (2) Lateral symmetry by paired side placement next to ensure balanced stereo imaging free of dead zones. (3) Front-back balance through distributed placement also optimizes Early/Later energy ratios.

The most common configuration, recommended in guidelines for angular distributions, uses 120° between all units to achieve clarity during performances audible over a range of speech-based sound levels. Small angular deviations ($\pm 10\text{--}15^\circ$) enhance spatial homogeneity for orchestral-type performances while decorrelating reflections and minimizing the formation of standing waves. Using extreme angles of 60° and 180° should be reserved for use cases where only one device is deployed and maximum directivity/coverage is required.

5.3. Economic and Logistical Optimization

The economic analysis leads to specific optimization strategies for resource-constrained implementations. Half an Hour Each: highest marginal improvement for single devices; levels of professionalism only acceptable in educational demonstrations/amateur performances (20% gain at

baseline cost) The two-device setups get you to an acceptable cost-efficiency ratio (30% gain for $2\times$ cost = 15% efficiency) might be fine for underserved community venues where it is more important to deliver the audio basics than have perfect acoustics.

For commercial deployments, both device types were found to deliver similar best investment (32–36% gain at $2\times$ cost for prawns and 38–43% gain at $3\times$ cost for professional venues, with the efficiency of these options being respectively 12.7–14.3% in additional catch benefit/head. This configuration aligns with industry standards, which recommend investing 2–5% of the overall construction cost in acoustic treatment^[7]. Break-even analysis reveals that it would require recouping an investment after 15–20 performances versus renting an electronic enhancement system, or after 40–50 performances for purchasing basic sound reinforcement equipment.

The complex structure of the poorer economic returns for 4 or more devices (>11% inefficient). Storage requirements increase from 6 m³ to 12 m³; setup time doubles from 30 minutes to 75 minutes, and maintenance scheduling becomes a problem as the number of failure points increases. For regular venues, that 5% of (small) performance boost is simply not worth the practical burdens.

However, multiple factors strongly support the design of devices in threes as you will see later in these mailing blog posts. Vehicle transportation (devices nest and transport at 2m × 1m × 0.5m per unit, so they fit within the backs of standard cargo vans or small trucks). Designed for two technicians to set up the software in 30 minutes or less. Ideal for venue changeover windows between shows. The visual impact is fine for standard stages, where they resemble the ornamental screens or acoustic shells associated with the minds of audiences. Maintenance schedule is easily achieved during standard venue operations, which includes quarterly inspection and annual deep cleaning; it takes 12 hours (maintenance) a year vs. over 40+ hours for electronics systems.

5.4. Cultural and Aesthetic Considerations

In addition to optimizing quantitatively, the multi-device approach provides unique cultural and aesthetic benefits. By deploying it at scale, this allows for a gradual "translation" between Eastern and Western acoustic traditions based on the number of devices at a location (acting as a cultural slider). Single devices preserve the cultural identity of the original space, while requiring minimum adaptation to foreign repertory. Neither device achieved balanced biculturalism, which would be the ideal condition for fusion performances where Eastern and Western music are mixed. The full cultural transformation demands all three devices while maintaining an architectural presence required for touring companies, which can present a full operatic or symphonic programme.

Replicable devices create an almost theatrical ambiance in which the fan-shaped forms, resembling both Chinese decorative screens and Western acoustic shells, dominate. Not only does this dual cultural reference enhance the subject with some universal soul, but it also caters to audiences across borderlines by preventing them from developing any inertia that might have been sown due to mere functional acoustic treatment. Devices are now included as part of the performance aesthetic rather than technical intrusions, with some venues requiring lacquer finishes and decorative patterns that echo architectural themes.

From a technical standpoint, the modular approach also opens up the possibility of participatory acoustics, where audience members can observe, for example, real-time acoustic adjustments during an educational concert. The visuals of simultaneously integrating more devices are a great way to dig into acoustic principles, encouraging music education. This transparency is a far cry from the "black box" electronic systems to which most Americans are exposed and about which they learn little.

5.5. Limitations and Boundary Conditions

While multi-device optimization offers strong solutions for all purposeful venues, a few restrictions raise an argument to be acknowledged. Only through the incorporation of new passive devices will their fundamental architectural limitations, such as a perfect sine wave power factor, be eliminated. Boston Symphony Hall and Listening Rain Pavilion have a volume ratio of 35:1, a near-impossible extreme for even the most ambitious number of devices to span. Even in the most impactful venue transformations, the maximum achievable RT60 modification is well-bounded at around $\pm 50\%$ relative to baseline, so it's not a complete venue type switch under any circumstance.

This all assumes perfect device placement, which is rarely possible given practical constraints such as sight lines, fire exits, stage access, and spaces for the performers. In the real world, venues are usually asymmetric, with acoustic shadows created by features such as balconies, columns, and seating that devices cannot reach. The study quantified (0-4 devices), but not the fractional contributions from partially active devices or variable-intensity operation that may allow tuning for specific frequency ranges.

However, the study did not entirely account for the presence of nonlinear effects in loud sound pressure levels (>100 dB), such as those found in an orchestral fortissimo or any operatic climax. The operation at extreme amplitudes must be avoided because device membranes can exhibit nonlinear behavior, with parametric effects and intermodulation distortion. For bamboo and paulownia (organic) materials, long-term stability under various humidity conditions should be normalized by our testing periodicity. Materials age and mechanical tolerances change, so coupling coefficients can drift over time.

5.6. Future Research Directions

The successful showcase of three-device optimization paves the way for further exploration. Device networks could collectively adapt in real-time configuration adjustments guided by acoustic feedback, thereby potentially enabling optimal performance across different segments of the repertoire. Machine learning algorithms can monitor audio streams and adjust fan angles — even device locations — between movements in a musical piece, thus achieving piece-specific optimization that is impossible with static configurations.

Investigating hybrid approaches that utilize different types of devices optimized for each frequency range may be warranted. Membrane absorbers can be used in conjunction with diffusive high-frequency devices to work together, both under the umbrella of integrated control systems that manage their operation. Stadium-scale (>> 10,000 seats) venue deployments could further investigate whether optimization principles based on traffic densities translate to extreme scale, or if new phenomena emerge at larger quantities.

AGVs equipped with smart positioning systems would enable dynamic repositioning of devices between prompts. This flexibility would let a single venue adapt to very different repertoires. Building management systems can utilize this technology to adjust device settings in response to HVAC operations, lighting, and audience occupancy, thereby achieving integrated environmental optimization.

If multiple devices are involved, two of these instructions relate to what is called psychoacoustic validation — a series of tests to determine if improvements in performance can actually be heard by listeners as the measured quantity increases. Perceptual scaling may not map physical measurements exactly, and improvements might cluster around perceptual thresholds in a more categorical manner. Cross-cultural listening tests may identify cultural differences in acoustical preference that could necessitate culture-dependent optimization strategies.

6. Conclusions

In this way, we have provided a more comprehensive description of multi-device acoustic resonator systems that illustrates the necessity of the parameter device number to achieve successful optimization in crossing the well-known dramatic Acoustic Gap Origo between Far Eastern and Western performances. After performing an exhaustive evaluation of 0-4 device configurations in two canonical venues (within the realistic parameters defined by a specific device operating distance) — Boston Symphony Hall and the Listening Rain Pavilion, robust optimization curves for deployment in practice were developed while developing a detailed understanding of how these devices shape sound within acoustic treatment systems.

For all metrics, the research definitively determines that three strategically placed devices are the optimal configuration. This reduces RT60 from 1.86s to 1.06s, and increases clarity C80 by up to +11.2 dB, while still complying with the target reverberation of 0.9-1.2s for Western halls and achieving a similar sound ($RT60 \approx 3s$) in theatres in China hosting Chinese opera using other forms

of seating such as chairslingtonium CMN cobble cement-bonded particle board. The control room often required on-stage musicians' specific logistics, seating areas, and Fixed-Tip Seats, or a combination of the two, known as a model house (e.g., Arabian dining). On the contrary, three devices in Eastern pavilions give 511% RT60 increase (0.18s to 1 Western symphonic music (ca 10s), providing reverberation that is necessary for harmonic development and orchestral blending. Spatial uniformity enhancements achieved a 39% improvement (CV declined from 18.3% to 11.2%), with cost-performance peaking at a 14.3% increase in performance per invested unit.

The underlying non-linear mathematical relationships observed in our device quantity versus acoustic improvement measurements are also straightforward to interpret, as exponential RT60 gain asymptotically plateaus [$\Delta RT = A - A(1 - e^{(-n/\tau)})$], sigmoid disc clarity improvements increase saturationily [$180 = (12/(1 + e^{(-2(n-2))}))$], and logenewise uniformity improve logarithmically with device count [CV reduction = $100 \times (7 \times \ln(n+1)\%)$]. This establishes a critical ratio of device area to room surface area ($A_d/A_s \approx 0.02-0.03$ for optimal performance) for evidence-based deployment decisions in untested venues using dimensionless scaling parameters.

Contributions to the science and practice of acoustics include: 1) establishing device quantity as an independent optimization parameter with predictable scaling laws; 2) identifying a three-device optimum that reconciles performance, cost, and logistical constraints across a broad range of venue types; 3) confirming theoretical tradeoffs between single distributed treatment versus large interventions through both analytical models and field measurements; 4) constructing frequency-dependent coupling models for multi-resonator systems addressing key mechanisms responsible for improvement through constructive interference; 5) deriving practical deployment guidelines to incorporate real-world constraints including sight lines, stage logistics, audience response feedback, as well as visual aesthetics.

Passive, non-electronic examples of this acoustic mediation make possible the first performances of traditional musics from around the world, which preserve their essential cultural authenticity, while allowing them to participate in a degree of cross-cultural musical interchange hitherto impossible. That the three-device configuration has emerged more as an actual optimum than an empirical one suggests this might be a fundamental balance point between coverage and no interference, excitation and control, and investment and return. This principle of optimization seems quite general, as even if test venues differ by 35 times in volume (because the -135 dB SPL frequency content does not change), performance spaces varying from small recital halls to large opera houses should benefit.

In acoustic engineering, these implications are as far-reaching as they are profound: indeed, cultural preservation and artistic exchange depend upon decisions such as who gets to listen to what in which circumstances. An optimized multi-device system that enables Chinese opera to be performed with authenticity in Western concert halls and Western symphonies to be showcased in Eastern gardens can function as a technological bridge between cultural practices. This scalable, modular strategy democratizes acoustic performance, making it feasible to add acoustical excellence incrementally based on budget and flexibility needs, supporting a wide variety of program types.

More computing power isn't necessarily bad, of course, but if there's a hard choice to be made in practice, it should be between achieving an optimal three-device configuration or one that includes more units. The resources spent on a fourth device would be better invested in some higher-quality components, professional positioning optimization, or dedicated training for the venue staff. These plots have established optimization curves that provide specific direction in these areas, and for the first time, there are guidelines that transform acoustic treatment from an empirical art into a predictive science.

The research is flagging a new paradigm in cross-cultural acoustic design, grounding technology among tradition rather than trumping it. This convergence between Eastern materials, Western acoustic fundamentals, and modern computational design provides a viable example of how innovation does not necessarily have to compromise authenticity. The acceleration of global cultural exchange underscores the necessity for acoustic solutions that both preserve and respect particular musical traditions, as well as afford an understanding and resonance across cultural divides. This three-device configuration, optimized for worldwide consistency yet global flexibility, creates the

tools necessary to meet this challenge with practical solutions that help maintain acoustic excellence worldwide in our connected and ever-diverse musical realm.

References

- [1] Lachenmayr, W., Meyer-Kahlen, N., Gomes, O. C., Kuusinen, A., & Lokki, T. (2023). Chamber music hall acoustics: Measurements and perceptual differences. *The Journal of the Acoustical Society of America*, 154(1), 388-400.
- [2] Al-Dabbagh, A. N., Kadhum, M. A., & Ali, S. H. (2024). Optimizing acoustic design for dual-function concert and speech halls. *Scientific Reports*, 14(1), 23456.
- [3] Trematerra, A., Iannace, G., & Amadasi, G. (2025). Acoustic shell optimization in opera houses for concert halls. *Applied Sciences*, 15(11), 5943.
- [4] Błasiński, Ł. (2025). Enhancing concert hall acoustics: The impact of acoustic banners and curtains. *Applied Acoustics*, 214, 110720.
- [5] Wang, X., Li, M., & Zhang, Y. (2025). Acoustic adaptation mechanism of a traditional ancestral temple theatre in northeast Jiangxi. *npj Heritage Science*, 13, 45.
- [6] Karaman, O. Y., & Çalışkan, M. (2025). Objective and subjective acoustic assessment of music halls with passive variable systems: A case of Bilkent Music Hall. *Applied Acoustics*, 231, 110720.
- [7] Ribeiro, D., Morgado, A., & Mateus, D. (2021). On the use of perforated sound absorption systems for variable acoustics room design. *Buildings*, 11(11), 543.
- [8] Pinto, F., & Cardoso, J. (2021). Variable acoustics in performance venues: A review. *Journal of the Acoustical Society of Korea*, 40(6), 523-538.
- [9] Le Goff, N., & Schmich, I. (2020). Variable acoustics, from design to everyday practice: Can it really work? *Proceedings of Forum Acusticum*, 2020.
- [10] Li, C. (2025). The integration and innovative practice of intelligent AI and local opera in college teaching. *Frontiers in Psychology*, 15, 1521777.
- [11] Li, Y. W., & Wan, L. C. (2024). When intangible cultural heritage meets modernization: Can Chinese opera with modernized elements attract young festival-goers? *Tourism Management*, 106, 104969.
- [12] Wen, X., Chen, Y., & Liu, H. (2022). Acoustic parameters analysis in Peking Opera theaters: Optimization for learning environments. *Building Acoustics*, 29(3), 245-262.
- [13] Chen, L., Wang, S., & Xu, M. (2022). Classification of styles in Cantonese opera singing using AI: Safeguarding intangible cultural heritage. *Journal of Cultural Heritage*, 58, 142-153.
- [14] Cox, T., & d'Antonio, P. (2020). *Acoustic absorbers and diffusers: Theory, design and application* (3rd ed.). CRC Press.
- [15] Asdrubali, F., & Pispola, G. (2020). Properties of transparent sound-absorbing panels for use in noise barriers. *The Journal of the Acoustical Society of America*, 121(1), 214-221.
- [16] Zhang, X., & Wang, X. (2023). Sustainable acoustic materials from natural fibers for architectural applications. *Building and Environment*, 228, 109876.
- [17] Kuttruff, H. (2016). *Room acoustics* (6th ed.). CRC Press.
- [18] Vorländer, M. (2020). *Auralization: Fundamentals of acoustics, modelling, simulation, algorithms and acoustic virtual reality* (2nd ed.). Springer.
- [19] Scheibler, R., Bezzam, E., & Dokmanić, I. (2018). Pyroomacoustics: A Python package for audio room simulation and array processing algorithms. In *2018 IEEE International Conference on Acoustics, Speech and Signal Processing (ICASSP)* (pp. 351-355).

- [20] Allen, J. B., & Berkley, D. A. (1979). Image method for efficiently simulating small - room acoustics. *The Journal of the Acoustical Society of America*, 65(4), 943-950.
- [21] Lehmann, E. A., & Johansson, A. M. (2008). Prediction of energy decay in room impulse responses simulated with an image-source model. *The Journal of the Acoustical Society of America*, 124(1), 269-277.
- [22] ISO 3382-1:2009. Acoustics — Measurement of room acoustic parameters — Part 1: Performance spaces. International Organization for Standardization.
- [23] Saaty, T. L. (1990). How to make a decision: The analytic hierarchy process. *European Journal of Operational Research*, 48(1), 9-26.
- [24] Sabine, W. C. (1922). *Collected papers on acoustics*. Harvard University Press.
- [25] Schroeder, M. R. (1987). Statistical parameters of the frequency response curves of large rooms. *Journal of the Audio Engineering Society*, 35(5), 299-306.
- [26] Nutter, D., & Gee, K. (2021). Modal analysis of coupled acoustic spaces: Theory and experimental validation. *The Journal of the Acoustical Society of America*, 149(3), 1823-1836.